Supporting Information

Unified Understanding of Ferroelectricity in *n*-Nylons: Is the Polar Crystalline Structure a Prerequisite?

Zhongbo Zhang, Morton H. Litt*, and Lei Zhu*

Department of Macromolecular Science and Engineering and Department of Chemistry, Case Western Reserve University, Cleveland, Ohio 44106-7202, United States

* Corresponding author. Tel.: +1 216-368-5861; Fax: +1 216-368-4202
E-mail addresses: lxz121@case.edu (L. Zhu) and mhl2@case.edu (M. H. Litt)

I. Temperature Dependent 1D WAXD Profiles for Various Nylon 12 Films

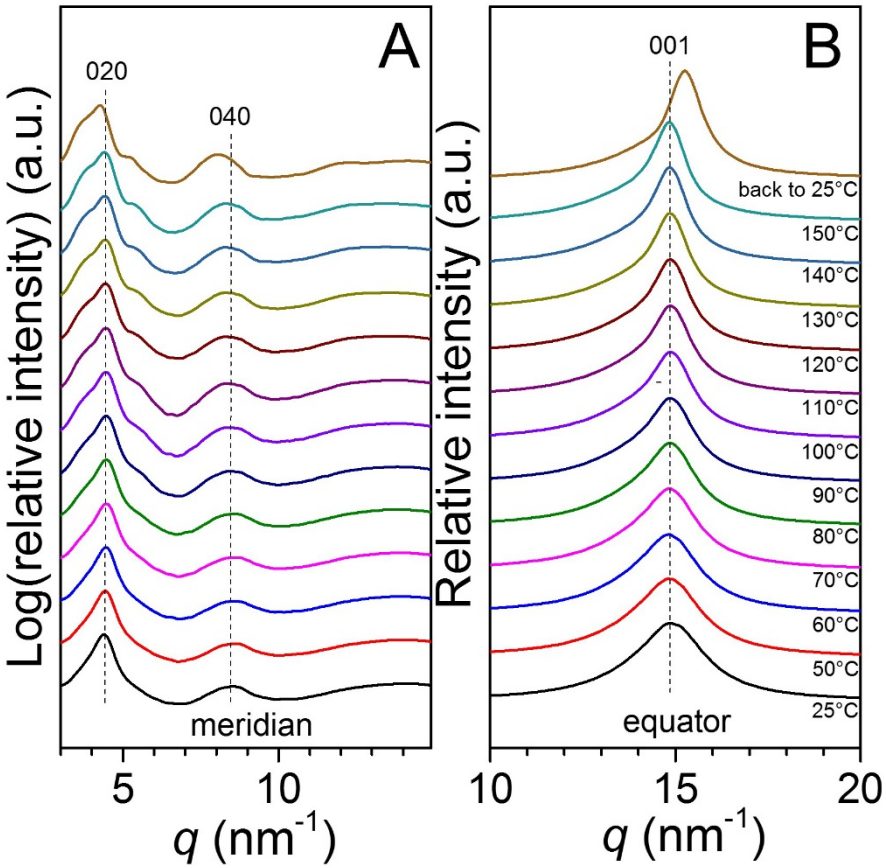

Figure S1. Temperature dependent 1D WAXD profiles for the QS nylon 12 film along (A) the meridian and (B) the equator directions in the corresponding 2D WAXD patterns. Peak assignments are shown in both plots.

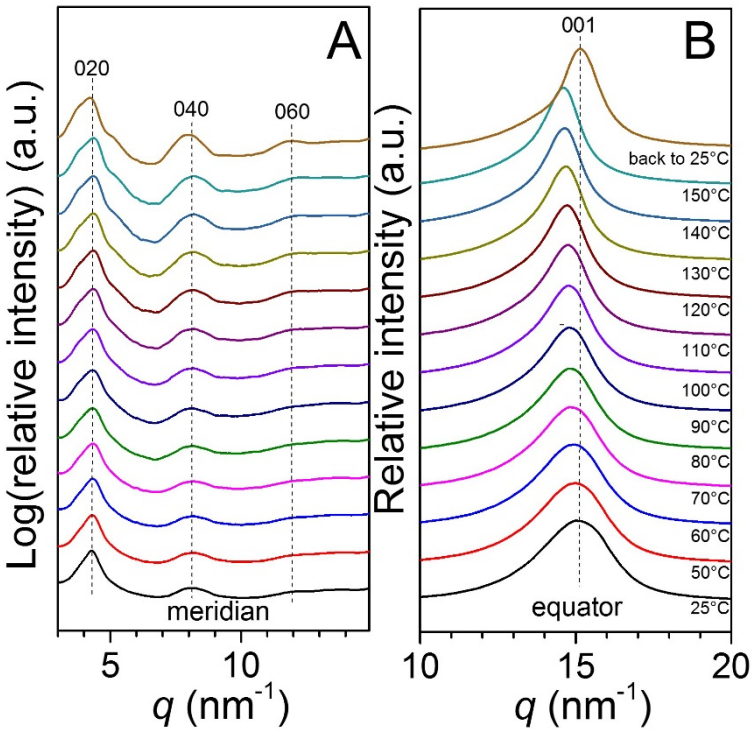

Figure S2. Temperature dependent 1D WAXD profiles for the QAS nylon 12 film along (A) the meridian and (B) the equator directions in the corresponding 2D WAXD patterns. Peak assignments are shown in both plots.

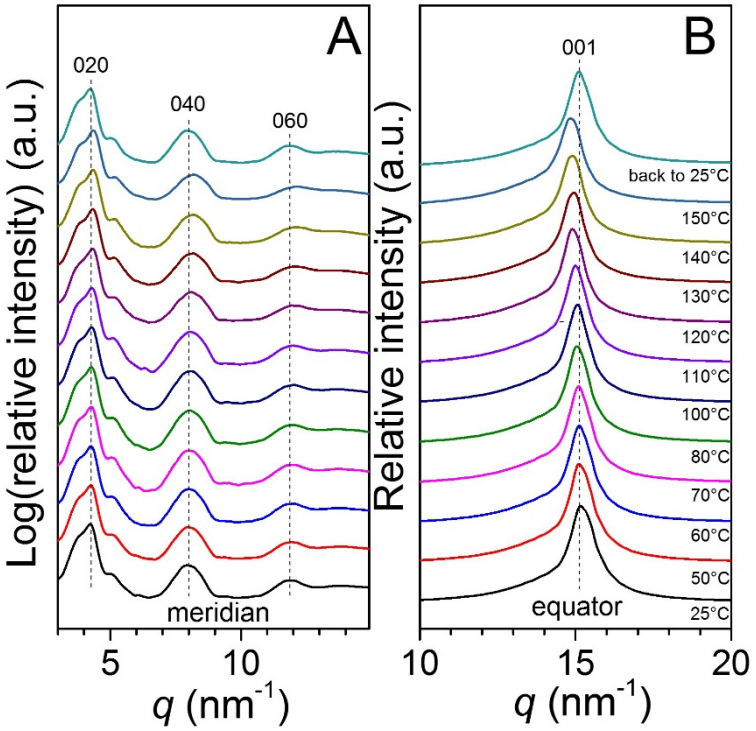

Figure S3. Temperature dependent 1D WAXD profiles for the QSA nylon 12 film along (A) the meridian and (B) the equator directions in the corresponding 2D WAXD patterns. Peak assignments are shown in both plots.

II. High-Field Bipolar D-E Loops for the Quenched, Stretched, and Annealed Nylon 12 Film

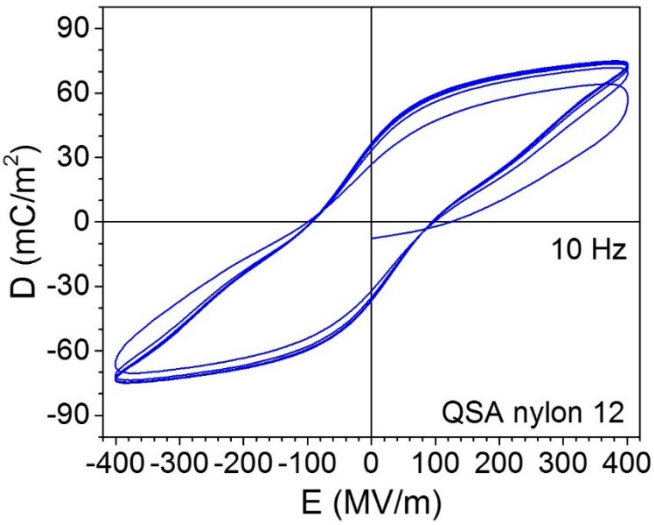

Figure S4. Continuous bipolar D-E hysteresis loops for the QSA nylon 12 film with the maximum poling field of 400 MV/m at room temperature and 10 Hz.

III. BDS Results for Quenched and Stretched Nylon 12, Nylon 6, and Nylon 11 Films

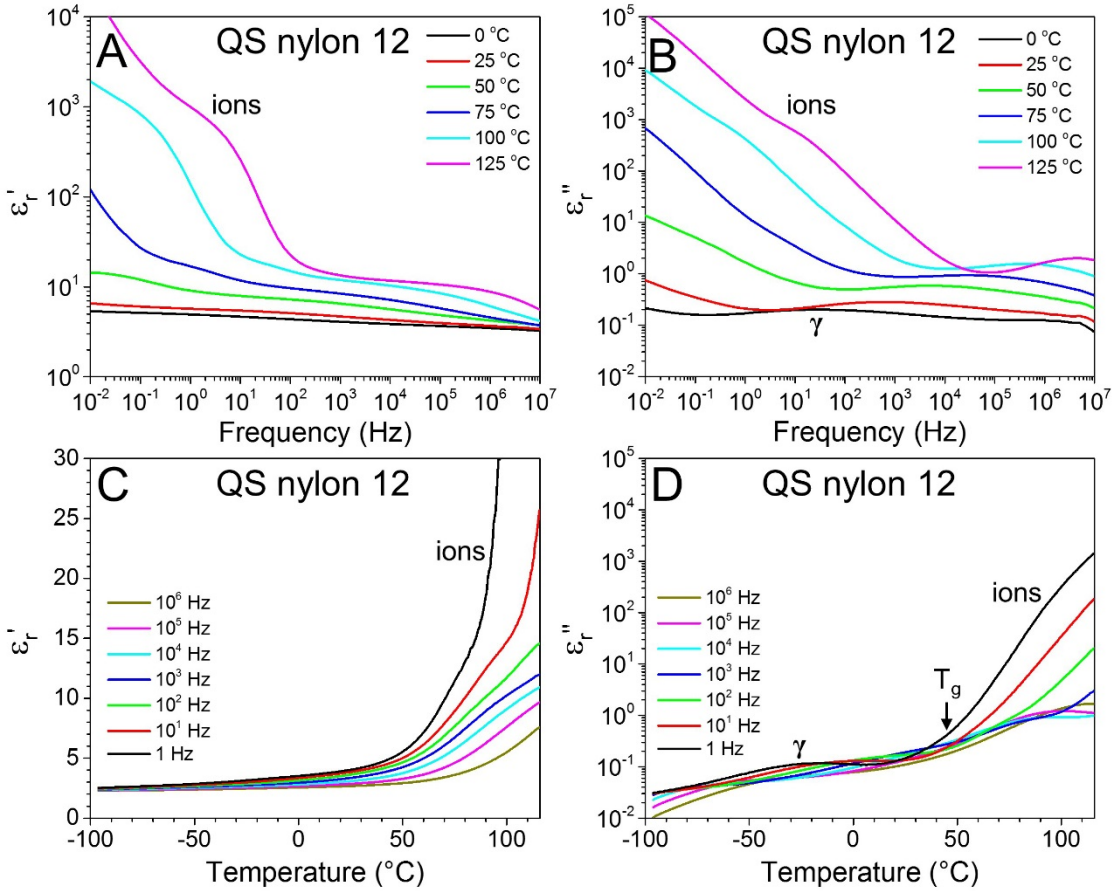

Figure S5. Frequency-scan BDS results, (A) ε_r' and (B) ε_r'', for the QS nylon 12 film. Second heating temperature-scan BDS results, (C) ε_r' and (D) ε_r'', for the QS nylon 12 film.

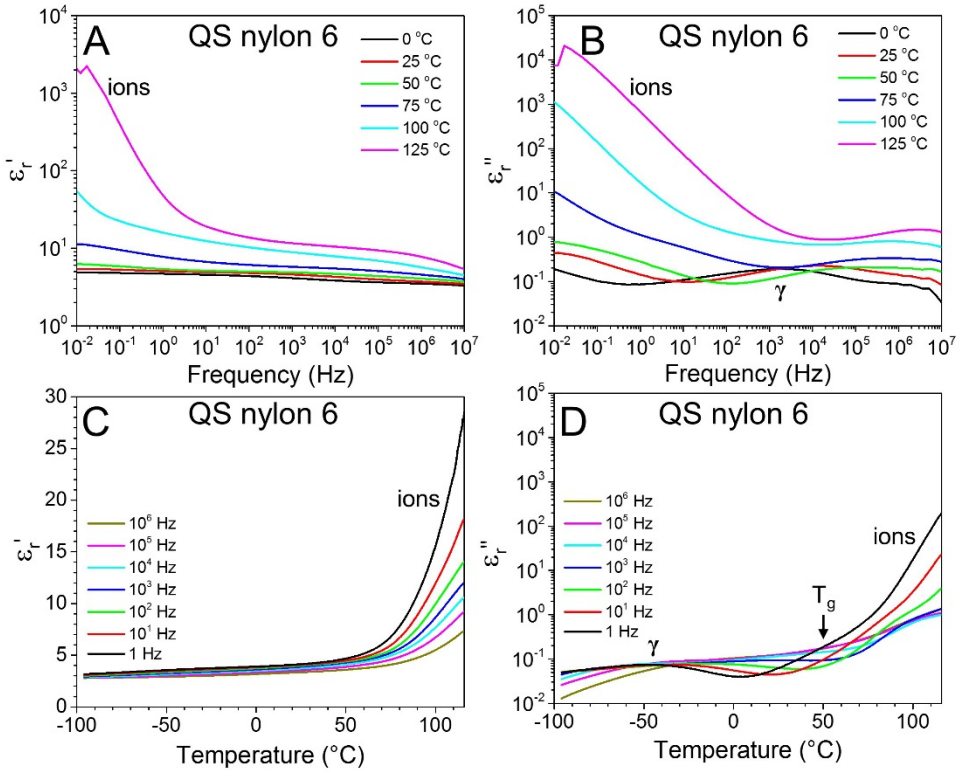

Figure S6. Frequency-scan BDS results, (A) ε_r' and (B) ε_r'', for the QS nylon 6 film. Second heating temperature-scan BDS results, (C) ε_r' and (D) ε_r'', for the QS nylon 6 film.

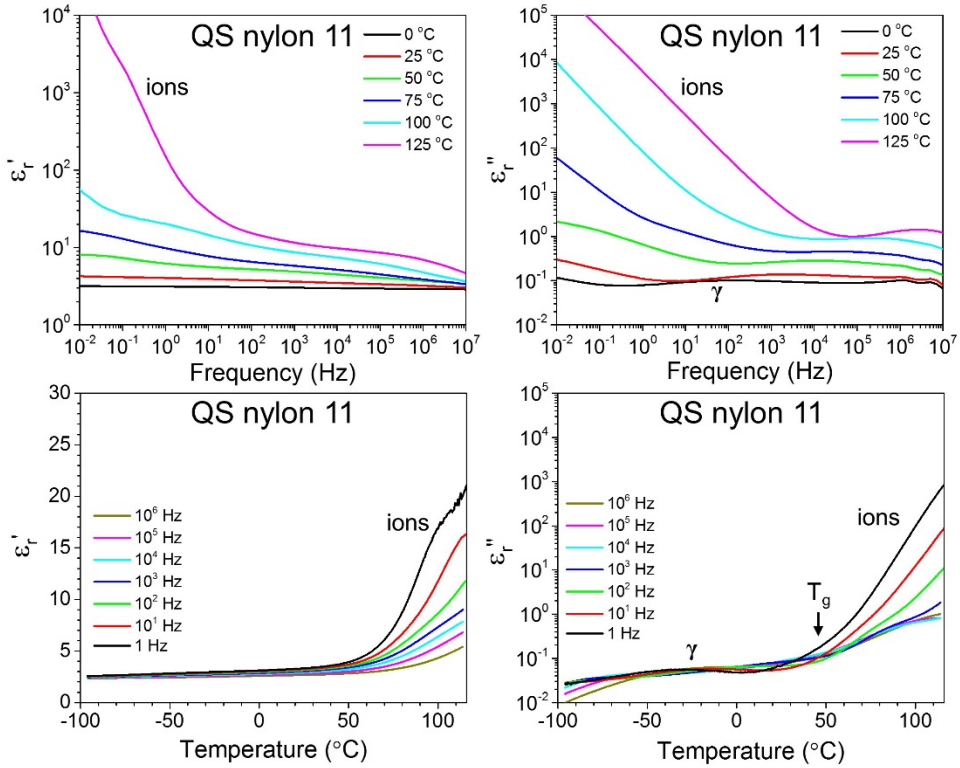

Figure S7. Frequency-scan BDS results, (A) ε_r' and (B) ε_r'', for the QS nylon 11 film. Second heating temperature-scan BDS results, (C) ε_r' and (D) ε_r'', for the QS nylon 11 film.

From the frequency-scan BDS results for the QS nylon 12, 6, and 11 films, significant impurity ion migrational loss is observed above the T_g around 50 °C below 10 Hz, as evidenced by both increases in ε_r' and ε_r'' at low frequencies. Comparing the impurity ion migrational losses among nylons 12, 6, and 11, nylon 6 has the lowest loss and thus the lowest amont of impurity ions. It is considered that the nylon 6 is synthesized by the ring-opening polymerization of caprolactam and nylons 12 and 11 are made by regular condensation polymerization. Therefore, nylons 12 and 11 contain more impurity ions than nylon 6. In addition, the γ relaxation processes in the amorphous phase are also observed for these samples, and their peak frequencies increase with increasing temperature.

In the temperature-scan BDS results for the QS nylon 12, 6, and 11 films, the γ relaxation processes in the amorphous phase are observed; around -50 °C for nylon 6 and around -30 °C for nylons 12 and 11. Above the T_g near 50 °C, significant impurity ion migrational losses are observed, especially at low frequencies. From both results, the impurity ion migrational losses are fairly low for the QS nylon 12, 6, and 11 samples at room temperature (RT) and 10 Hz.

IV. Comparison of Remanent Electric Displacement for Quenched and Stretched Nylon 11 and Nylon 12 Films

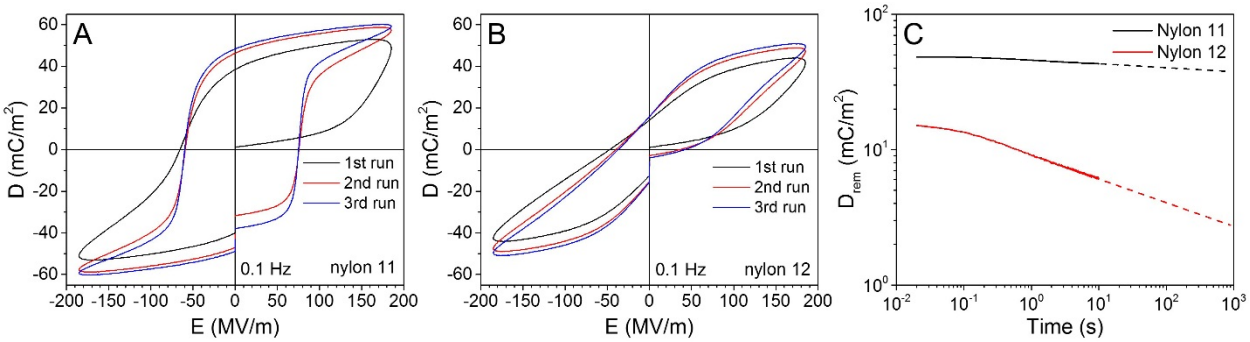

Figure S8. Room temperature bipolar D-E loops for (A) the QS nylon 11 film and (B) the QS nylon 12 film at room temperature, respectively. The poling frequency is 0.1 Hz. (C) D_{rem} as a function of time after the third run for the QS nylons 11 and 12, respectively. The dashed lines are extrapolation to longer times.

The D_{rem} as a function of time was studied after three consecutive bipolar D-E loops runs. Figures S8A and B show the bipolar D-E loops at 0.1 Hz and room temperature for the QS nylons 11 and 12 films at 0.1 Hz and room temperature, respectively. The time interval in between the consecutive runs was about 30 sec. The D_{rem} as a function of time after the third run for the QS nylons 11 and 12 are shown in Figure 8C. The D_{rem} for the QS nylon 12 film was lower than that for the QS nylon 11 film. More importantly, the decrease of D_{rem} for the QS nylon 12 film was more dramatic than that for the QS nylon 11 film. From this result, we concluded that the electric field-induced ferroelectric domains in the QS nylon 12 were smaller and less stable than those in the QS nylon 11. From our previous study,[S1] homocharge injection and polarization of impurity ions can be ignored for nylon 11 and 12 at room temperature. Therefore, the decrease in D_{rem} is attributed primarily to the disorientation of ferroelectric domains.

V. Paraelectricity in the Amorphous Phase of *n*-Nylons

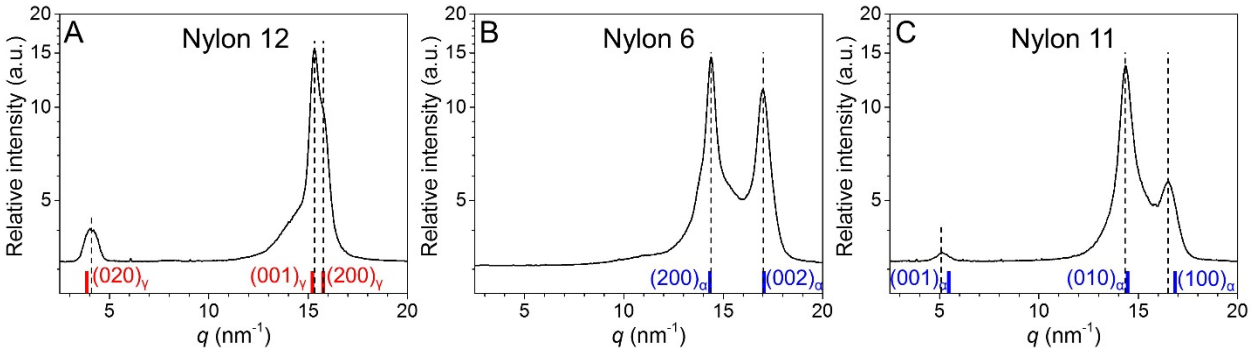

Figure S9. 1D WAXD profiles for hot-pressed nylon 12, nylon 6, and nylon 11 films isothermally crystallized at preset temperatures (140 °C for nylons 12 and 6 and 150 °C for nylon 11) for 12 h.

To determine whether the amorphous phases in nylons 12, 6, and 11 have ferroelectricity, the resins were hot-pressed in the melt (190 °C for nylon 12, 240 °C for nylon 6, and 210 °C for nylon 11) and isothermally crystallized at a preset temperature (140 °C for nylon 12 and 6 and 150 °C for nylon 11) for about 12 h, before slowly cooling back to RT. The 1D WAXD results in Figure S9 showed that these samples are almost completely in their most stable crystalline phases, i.e., the γ phase for nylon 12, the α phase for nylon 6, and the α phase for nylon 11, respectively. These hot-pressed films (about 30-50 μm thick) without any orientation were then subjected to bipolar D-E loop studies as shown below.

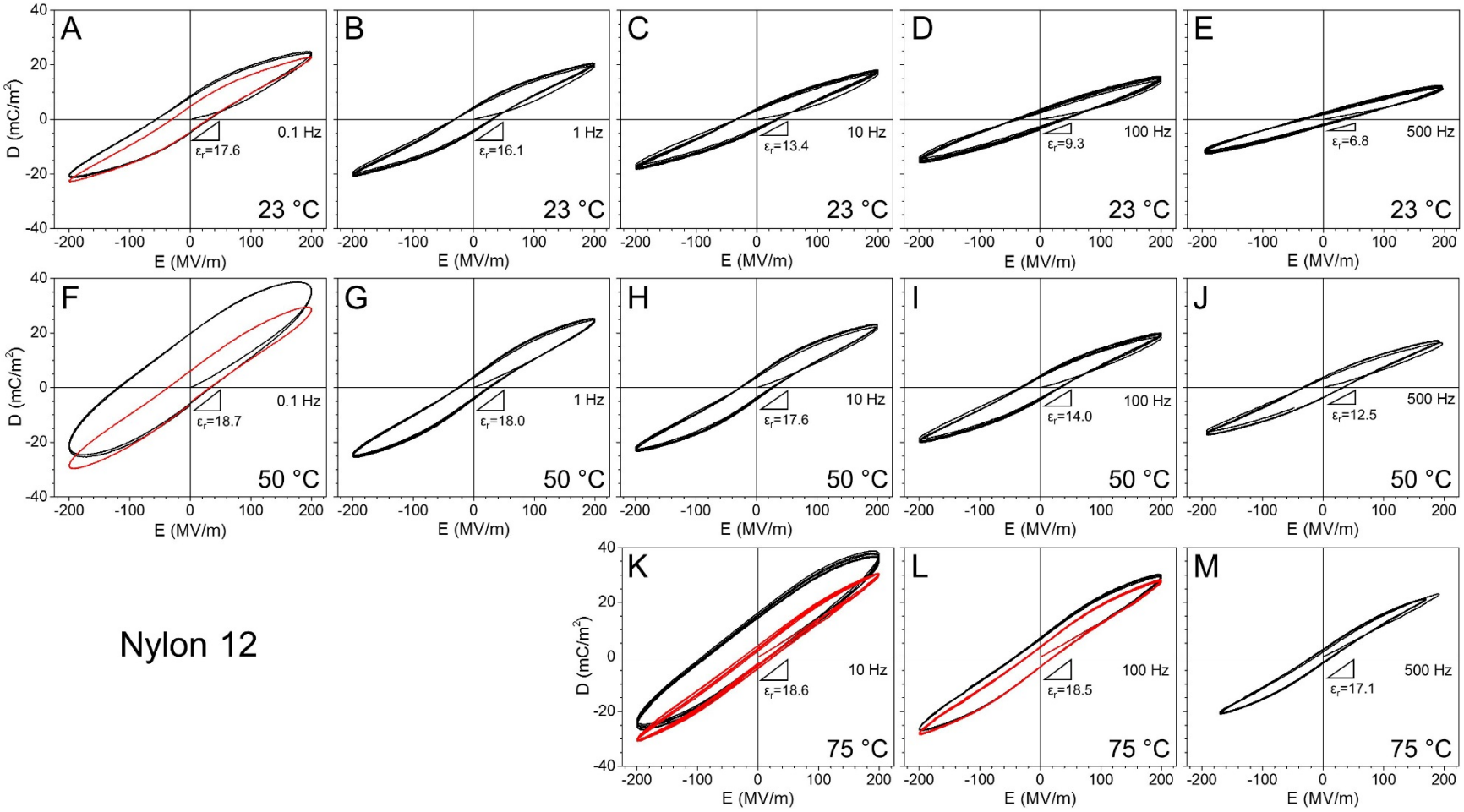

Figure S10. The third runs of continuous (2 loops for 0.1 Hz and 5 loops for the rest frequencies) bipolar D-E loops for the hot-pressed γ-phase nylon 12 film at (A-E) 23 °C, (F-J) 50 °C, and (K-M) 75 °C, respectively. The poling frequencies (sinusoidal wave function) are (A,F) 0.1 Hz, (B,G) 1 Hz, (C,H,K) 10 Hz, (D,I,L) 100 Hz, and (E,J,M) 500 Hz, respectively. The maximum poling field is set at 200 MV/m. At high temperatures and low frequencies, electronic conduction becomes significant and shifts the upper part of the D-E loop upward. After subtraction of the electronic conduction from the raw data (black loops),[S2] the red loops represent the hysteresis loops from both dipolar and ionic polarizations in the sample. Values of the apparent dielectric constant (ε_r) in the linear region are shown in the figures.

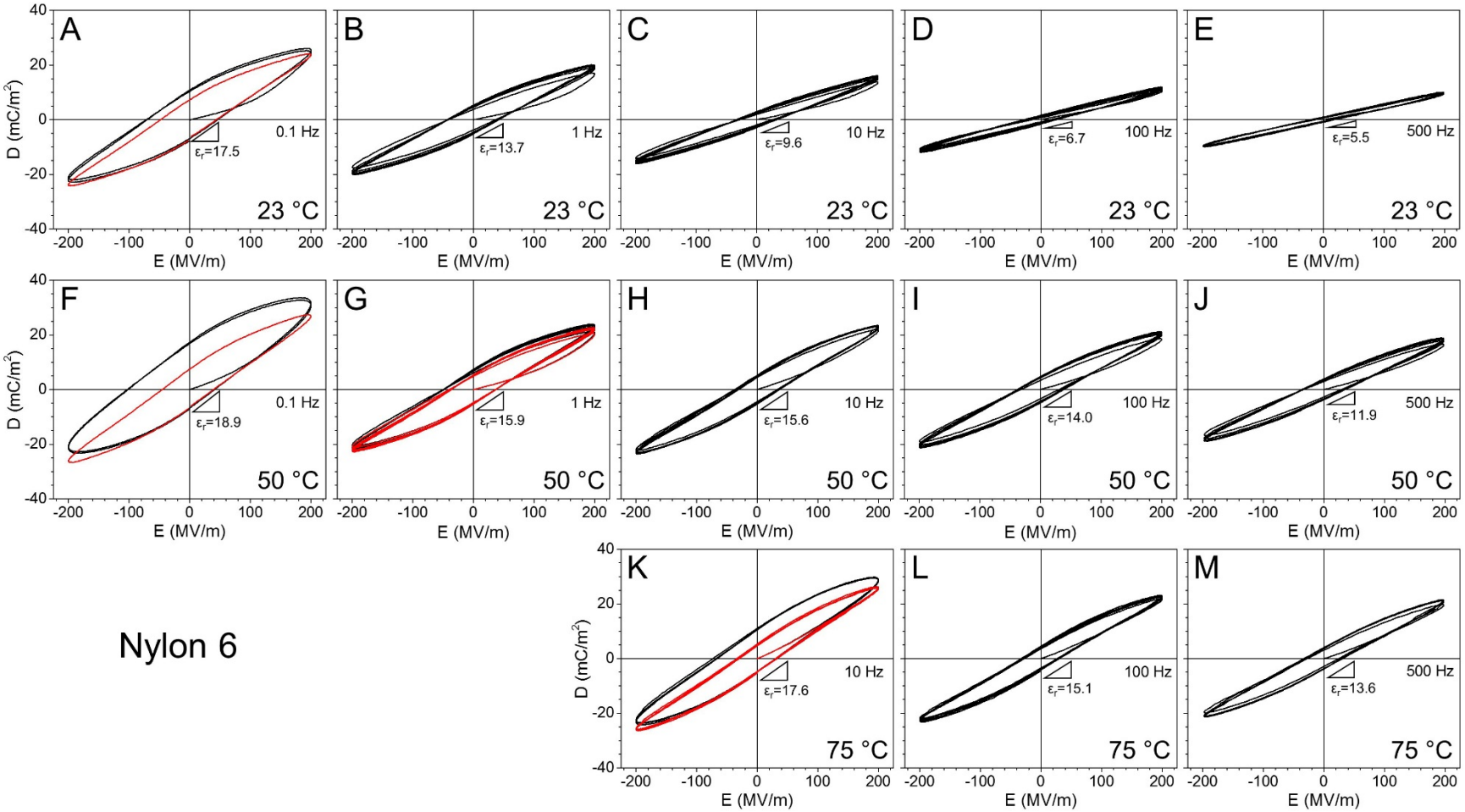

Figure S11. The third runs of continuous (2 loops for 0.1 Hz and 5 loops for the rest frequencies) bipolar D-E loops for the hot-pressed α-phase nylon 6 film at (A-E) 23 °C, (F-J) 50 °C, and (K-M) 75 °C, respectively. The poling frequencies (sinusoidal wave function) are (A,F) 0.1 Hz, (B,G) 1 Hz, (C,H,K) 10 Hz, (D,I,L) 100 Hz, and (E,J,M) 500 Hz, respectively. The maximum poling field is set at 200 MV/m. At high temperatures and low frequencies, electronic conduction becomes significant and shifts the upper part of the D-E loop upward. After subtraction of the electronic conduction from the raw data (black loops),[S2] the red loops represent the hysteresis loops from both dipolar and ionic polarizations in the sample. Values of the apparent dielectric constant (ε_r) in the linear region are shown in the figures.

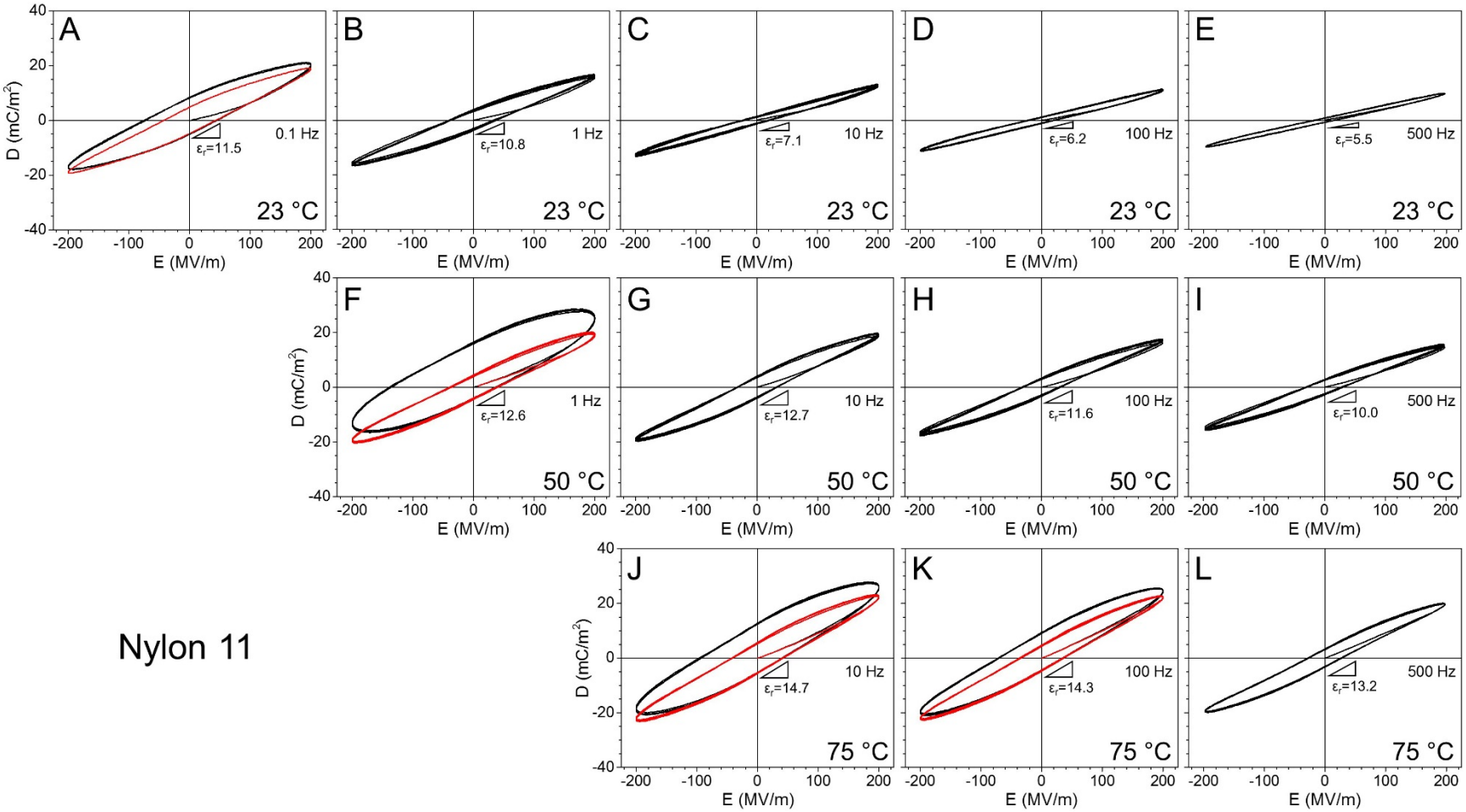

Figure S12. The third runs of continuous (2 loops for 0.1 Hz and 5 loops for the rest frequencies) bipolar D-E loops for the hot-pressed α-phase nylon 11 film at (A-E) 23 °C, (F-I) 50 °C, and (J-L) 75 °C, respectively. The poling frequencies (sinusoidal wave function) are (A) 0.1 Hz, (B,F) 1 Hz, (C,G,J) 10 Hz, (D,H,K) 100 Hz, and (E,I,L) 500 Hz, respectively. The maximum poling field is set at 200 MV/m. At high temperatures and low frequencies, electronic conduction becomes significant and shifts the upper part of the D-E loop upward. After subtraction of the electronic conduction from the raw data (black loops),[S2] the red loops represent the hysteresis loops from both dipolar and ionic polarizations in the sample. Values of the apparent dielectric constant (ε_r) in the linear region are shown in the figures.

It is known that the most stable crystalline forms of nylons 12, 6, and 11 do not exhibit any ferroelectricity due to the tight packing of strong H-bonding sheets. If there is any ferroelectricity, it should originate from the amorphous phases. For bipolar D-E loop studies, the hot-pressed nylon films were subject to three consecutive runs with each run comprised of either 2 (0.1 Hz) or 5 (1, 10, 100, and 500 Hz) continuous bipolar loops. The time interval between two consecutive runs was about 30 s. Three poling temperatures were chosen: 23 (RT), 50, and 75 °C. Note that RT is below the T_gs of nylons 12, 6, and 11, 50 °C is within the T_g range, and 75 °C is above the T_gs.

Above the T_g, amorphous polymers should exhibit paraelectricity rather than ferroelectricity, because the highly mobile amorphous dipoles (e.g., relaxation at $>10^5$ Hz for nylons 12, 6, and 11; see Figures S5A/B, S6A/B and S7A/B above) do not allow the formation and/or long lifetime of the spontaneous polarization (i.e., ferroelectric domains). This was exactly observed for the hot-pressed nylons 12, 6, and 11 films at 75 °C (Figures S10-S12). First, for nylon 11 at 75 °C (Figure S12), the apparent dielectric constant (ε_r), which is defined as the slope at low fields from -30 to 30 MV/m, slightly increased from 13.2 to 14.7 upon decreasing the poling frequency from 500 Hz to 10 Hz. Meanwhile, the loops gradually became broadened with increased dielectric nonlinearity. By definition, a paraelectric should not exhibit any dielectric nonlinearity in the D-E loop, because it does not contain any ferroelectric domains. The observed nonlinearity in the D-E loops at 75 °C could be attributed to the migrational loss of impurity ions in the sample; the lower the frequency, the higher the dielectric loss. Similar D-E loop broadening was also observed for paraelectric poly(vinylidene fluoride-*co*-trifluoroethylene) [P(VDF-TrFE)] above the Curie temperature below 100 Hz.[S3] Note that at high temperatures (and low frequencies), electronic conduction becomes significant in the sample and thus shifts the upper part of the D-E loop up (i.e., asymmetric with respect to the axis, D = 0).[S2] The electronic conduction should be subtracted in order to remove its contribution to the D-E loops (see the red loops after subtraction of electronic conduction in Figures S10-12). Second, at 75 °C the hot-pressed nylons 12 and 6 films exhibited similar hysteresis loops, but with higher ε_r values for different reasons. Nylon 6 exhibited a higher ε_r because of its higher dipole density. Nylon 12 exhibited a higher ε_r possibly because of the existence of a small fraction of poor γ crystallites which are polarizable by high electric fields.

Around the T_g, the hot-pressed nylons 12, 6, and 11 films exhibited similar hysteresis loops and the ε_r values slightly decreased compared to those above the T_g (Figure S10-12). Judging from the ε_r values and the loop shapes, again the electrical behavior can be attributed to paraelectric rather than ferroelectric. Below the T_g, it is hypothesized that the high electric field poling may lock in the spontaneous polarization or ferroelectric domains in the glassy state. However, D-E loop results at 23 °C in Figures S10-12 do not strongly support this hypothesis. Upon increasing the poling frequency, the paraelectric loops gradually became linear and the ε_r values significantly decreases. Even at a low frequency of 0.1 Hz, the ε_r values were fairly low for ferroelectric polymers, i.e., ~17.5 for nylons 12 and 6 and only ~11.5 for nylon 11. At ca. 25 °C below the T_gs, the hydrogen-bond dipoles (NOT ferroelectric domains!) could still be switched by high enough electric fields. Therefore, at RT *n*-nylons should still be considered as paraelectric rather than ferroelectric.

From the above studies, we conclude that the amorphous phases in *n*-nylons are not ferroelectric, but paraelectric in nature. The significant dielectric nonlinearity in D-E loops at low frequencies (e.g., 0.1 Hz) and high electric fields close to the T_g is attributed to both contributions from both impurity ions and the Brownian motion of amorphous dipoles, as we reported recently.[S4] Note that all these hysteresis loops are much slimmer than those observed for the mesomorphic

nylons 12, 6, and 11 films; see Figures 5, 7, 9, and 11 in the main text.

References

S1. Litt, M. H.; Hsu, C.-H.; Basu, P. Pyroelectricity and Piezoelectricity in Nylon-11. *J. Appl. Phys.* **1977**, *48*, 2208-2212.

S2. Yang, L.; Allahyarov, E.; Guan, F.; Zhu, L. Crystal Orientation and Temperature Effects on Double Hysteresis Loop Behavior in a Poly(vinylidene fluoride-*co*-trifluoroethylene-*co*-chlorotrifluoroethylene)-*graft*-Polystyrene Graft Copolymer. *Macromolecules* **2013**, *46*, 9698-9711.

S3. Su, R.; Tseng, J.-K.; Lu, M.-S.; Lin, M.; Fu, Q.; Zhu, L. Ferroelectric Behavior in the High Temperature Paraelectric Phase in a Poly(vinylidene fluoride-*co*-trifluoroethylene) Random Copolymer. *Polymer* **2012**, *53*, 728-739.

S4. Li, Y.; Ho, J.; Wang, J.; Li, Z.-M.; Zhong, G.-J.; Zhu, L. Understanding Nonlinear Dielectric Properties in a Biaxially Oriented Poly(vinylidene fluoride) Film at Both Low and High Electric Fields. *ACS Appl. Mater. Interfaces* **2016**, *8*, 455-465.